Proceedings of the ASME 2010 World Conference on Innovative Virtual Reality
WINVR2010
May 12-14, 2010, Ames, Iowa, USA

WINVR2010-3769

AUTOMATED WELD INTEGRITY ANALYSIS USING 3D POINT DATA

Matthew Swanson
Robotics Institute
Carnegie Mellon University
Pittsburgh, Pennsylvania 15213

Eric Johnson
Technology Innovations Center
John Deere
Moline, IL 61265

Alexander Stoytchev
Virtual Reality Applications Center
Iowa State University
Ames, Iowa 50011

ABSTRACT

This paper describes a method for non-destructive evaluation of the quality of welds from 3D point data. The method uses a stereo camera system to capture high-resolution 3D images of deposited welds, which are then processed in order to extract key parameters of the welds. These parameters (the weld angle and the radius of the weld at the weld toe) can in turn be used to estimate the stress concentration factor of the weld and thus to infer its quality. The method is intended for quality control applications in manufacturing environments and aims to supplement, and even eliminate, the manual inspections which are currently the predominant inspection method. Experimental results for T-fillet welds are reported.

INTRODUCTION

It is a common myth that manual welding in factories has been entirely displaced by robotic welding. While it is true that for large production volumes a robotic solution is commonly used, this technological investment cannot always be justified for small production volumes. Deploying a welding robot can easily cost as much as $1 million or even more in some cases. Therefore, even large companies continue to use human welders.

Even if cost were not a factor, there are still some structures that are simply too big to be welded by a robot. These structures have parts that are either too long or have welds in positions that can be difficult for a robot to reach. Some structures also contain many sub-components, which have to be manually positioned in place before they are welded. Thus, in many factories manual welding is still performed on a daily basis. It is unlikely that this situation will change anytime soon, which means that manual welding operations are likely to be a part of normal manufacturing processes for at least another decade. For this reason alone, it is useful to develop reliable and automated techniques for quality inspection of welds.

In the age of globalization quality control systems for weld inspection become even more important. While many large manufacturing companies have their own welding schools and routinely train their own welders to weld properly, it is becoming increasingly rare to find products that are welded from start to finish in the same factory. These days a product can contain parts that are welded across different countries and even continents. It is also becoming very common for products to be welded by more than one company, each with a slightly different quality control record. Sub-components welded by third-party suppliers are routinely integrated into finished welded assemblies. While outsourcing the welding of these sub-components may be cost efficient, the company that sells the finished product is ultimately responsible for the quality of the product. Therefore, it might be a good idea to invest in a system for automated weld integrity analysis.

Even if the welds are deposited properly and have no visible structural flaws it is still useful to inspect them using an automated system. For example, suppose that the part's blueprint calls for an 8mm weld at a certain location but the welder deposited only a 6mm weld. The 2mm difference may be quite difficult to detect with a naked eye (the typical inspection method). Furthermore, manually inspecting welded structures with multiple welds is often tedious and time consuming. The inspectors often fail to inspect all welds, especially if the parts contain thousands of welds. To counteract this, companies resort to 300% inspection levels (i.e., three different people inspect the same part one after another), which further increases the manufacturing costs.

This paper describes an automated method for non-destructive evaluation of the quality of welds. The method uses a high-end stereo camera system to capture the 3D geometry of

Copyright © 2010 by ASME

welds. The geometrical properties of each weld are analyzed using a computer program, which extracts the weld angle and the radius of the weld at the weld toe. These weld parameters can, in turn, be used to estimate the quality of each weld as shown in the next section. Experimental results for T-fillet welds are reported.

RELATED WORK

Previous research has shown that the durability of a welded structure is dependent on the geometry of the weld [1]. The relationship between the stress at the weld toe and the nominal stress (the stress far away from the weld toe) is expressed with the stress concentration factor K_t. This relationship is given by the following equation [1]:

$$\sigma_{peak} = K_t * \sigma_n$$

where σ_{peak} is the stress at the weld toe, K_t is the stress concentration factor, and σ_n is the nominal stress. K_t is dependent on the weld angle and the radius of the weld toe [1]. There are two K_t factors, K_t^b and K_t^m, which represent the bending stress and the membrane stress (or tension stress), respectively. The relationship between K_t^b, K_t^m and the weld geometry is given by the following equations:

$$K_t^b = 1 + 0.512 * \theta^{0.572} * \left(\frac{t}{r}\right)^{-0.469}$$

$$K_t^m = 1 + 0.388 * \theta^{0.37} * \left(\frac{t}{r}\right)^{-0.469}$$

where θ is the weld angle, r is the weld toe radius (in radians), and t is the thickness of the material (in millimeters).

While it is useful to know the mathematical relationship between the weld geometry and the durability of the weld, it is still difficult to extract weld geometry measurements automatically. In the past, we have successfully used dental molding to estimate weld geometry (see Figure 1). This method applies dental cement to the surface of welds in order to take a negative impression of the weld. Once the cement has set, it is cut into slices and the profiles are analyzed under a microscope.

The dental molding method can be very precise but it has several drawbacks. First, it is time consuming– it takes an experienced materials engineer approximately 1.5-2.0 hours to process a single weld. Second, this process can only be applied to a small number of welds and is impractical for large scale inspection of parts. In the past, this process has been used in a limited way to test only the most critical welds on a structure (see Figure 2). Third, for long welds only a small fraction of the welds can be covered by the molding. Fourth, the dental cement must be cut in order to be analyzed under a microscope. Because each slice has some thickness there is an upper limit to the number of slices that can be processed per weld (typically about 10).

Another weld measuring approach that we have used in the past relies on a specialized stereo vision system, which takes high-resolution images of a weld and produces a 3D model of its geometry (see Figure 5). While this approach is relatively fast compared with the dental molding approach it is still not fully automated. What is automated is the data measurement process (i.e., taking high-resolution images). However, the data analysis process (i.e., extracting the weld geometry parameters needed to estimate the stress concentration factor K_t) is still performed manually. The method described in this paper automates the entire weld analysis procedure.

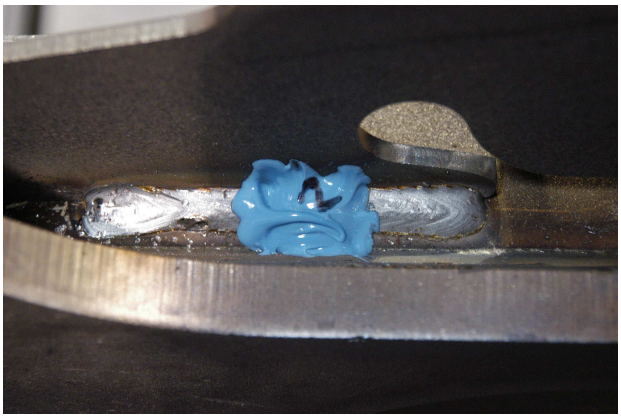

FIGURE 1. ONE PREVIOUS APPROACH TO WELD QUALITY ANALYSIS THAT USES DENTAL CEMENT MOLDING TO TAKE A NEGATIVE IMPRESSION OF THE WELD.

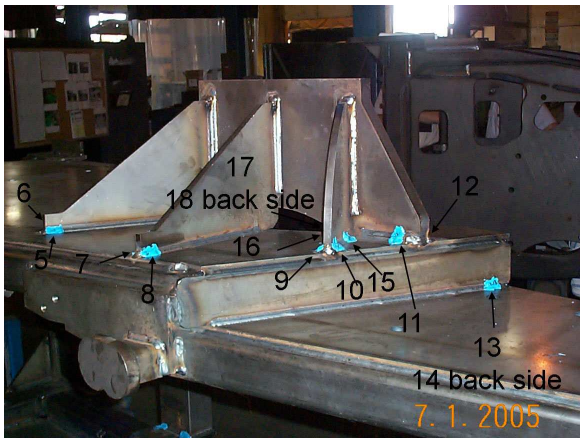

FIGURE 2. PREVIOUS APPROACH: MEASUREMENTS USING THE DENTAL MOLDING TECHNIQUE ARE TAKEN AT THE CRITICAL WELDS OF THE STRUCTURE.

EXPERIMENTAL SETUP

The experiments described in the next section compare the new 3D data scanning method for weld analysis with the old method that relied on dental molding. The experiments focus

Copyright © 2010 by ASME

on T-fillet welds, which are welds that connect two metal plates placed at right angles relative to each other (see Figure 3). T-fillet welds are commonly used in manufacturing. Figure 2 shows a large welded assembly with multiple T-fillet welds on it.

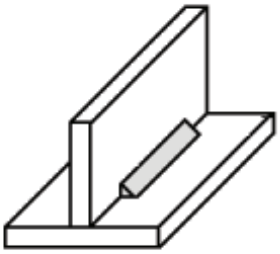

FIGURE 3. STYLIZED T-FILLET WELD.

The 3D profiles of the welds were scanned using an ARAMIS camera measurement system manufactured by GOM (see Figure 4). For each measurement, the ARAMIS system outputs a geometry file in STL format. The STL files were exported for computational measurements and converted to VRML files. The VRML files were then parsed and the 3D point data was processed using a Java program.

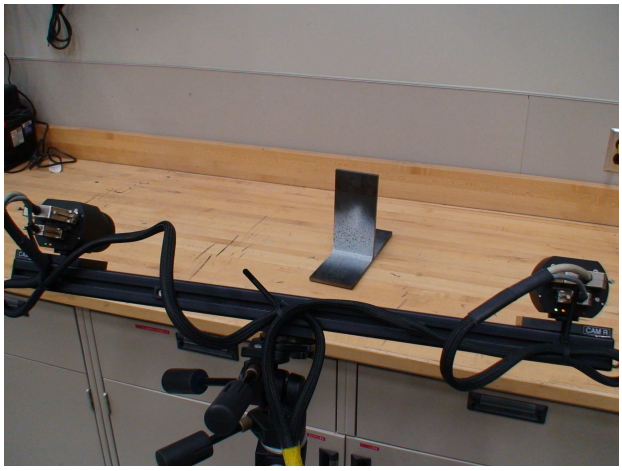

FIGURE 4. THE ARAMIS CAMERA SYSTEM THAT WAS USED TO GENERATE 3D WELD SCANS LIKE THE ONE SHOWN IN FIGURE 5.

ARAMIS uses image correlations to build the 3D representation of the weld. To improve the scanning resolution of the camera, it is useful to paint a stochastic pattern on the sample. This is done by painting a base coat of white followed by a black speckle pattern (see Figure 4). The system uses this random pattern to fit facets, which build the geometry. The system was calibrated using a 165 mm panel, which results in a resolution of 0.5 microns.

Figure 5 shows one of the virtual weld meshes produced by the ARAMIS system. Depending on the camera resolution that is used, the STL file can contain between 80,000 and 200,000 three-dimensional points, which is sufficient to capture even the smallest details of the weld geometry. The next section describes how this 3D data was processed to analyze the structural integrity of the weld.

EXTRACTING THE WELD PARAMETERS

This section describes the algorithm that was used to automatically extract the parameters of T-fillet welds. The algorithm takes as input a set of 3D points describing a single T-fillet weld (produced by the ARAMIS system described in the previous section) and outputs the parameters of the weld (weld angle and radius at the weld toe) at different locations along the length of the weld. These parameters can then be used to estimate the stress concentration factors K_t^b and K_t^m for the weld, which have been previously shown to be good predictors of weld quality.

The algorithm has three main stages: 1) detecting the weld and the two metal plates; 2) virtually slicing the weld; and 3) calculating the weld parameters. Each of the three stages is described in detail below.

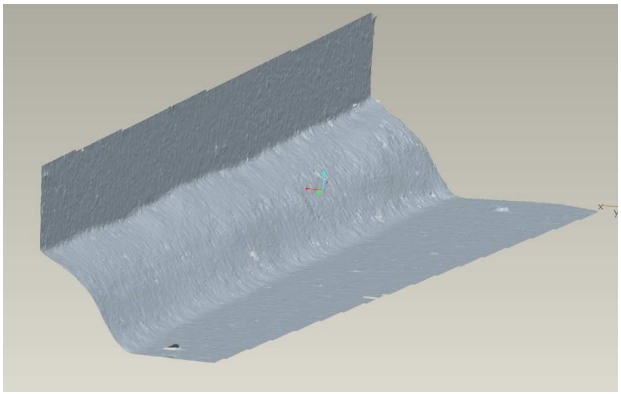

FIGURE 5. 3D MESH OF THE T-FILLET WELD SHOWN IN FIGURE 4. PARTS OF THE TWO METAL PLATES AND THE SURFACE OF THE WELD ARE CLEARLY VISIBLE.

Detecting the Weld and Metal Plates

The first step of the algorithm determines which 3D points from the scan belong to the weld and which points belong to the

Copyright © 2010 by ASME

two metal plates that are joined by the weld. This is done as follows.

First, surface normals are calculated for each 3D point from the weld scan. For each point, p, the algorithm finds its two closest neighbors (e.g., point q and point r), which are used to form two vectors:

$$\vec{u} = q - p$$

$$\vec{v} = r - p$$

The two vectors, $\vec{u}$ and $\vec{v}$, define a plane and their cross product defines the plane normal vector. This vector is used as an approximation for the normal to the surface of the entire weld at the point p.

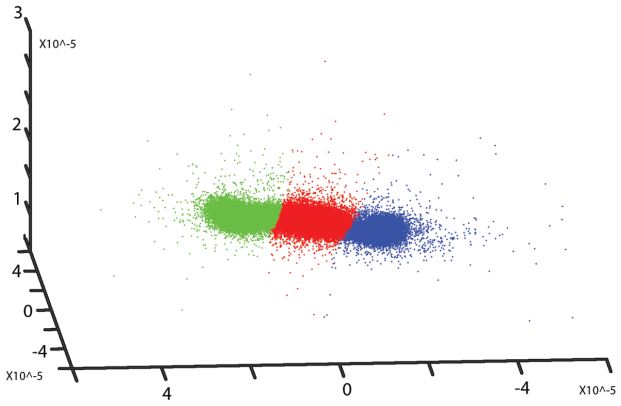

FIGURE 6. CLUSTERING RESULTS FOR THE SURFACE NORMALS OF ALL 3D POINTS FROM THE WELD SCAN SHOWN IN FIGURE 5. THE THREE CLUSTERS REPRESENT: METAL PLATE #1 (GREEN POINTS); METAL PLATE #2 (BLUE POINTS); AND THE WELD (RED POINTS). THESE CLUSTERS WERE GENERATED USING THE K-MEANS CLUSTERING ALGORITHM.

Second, the plane normals for all points in the weld scan are clustered using the k-means clustering algorithm [2]. Figure 6 shows the clustering results after running k-means with k=3 on the set of all unit normal vectors. Each point in the figure represents the normal vector at a 3D point. The three resulting clusters belong to the weld and the two metal plates (see Figure 7). The cluster means for each of the three clusters are used to identify the clusters as either one of the two metal plates or the weld. This is easy to do because the normals to the two metal plates differ from each other by approximately 90°. Thus, the remaining cluster must be the weld.

Third, for every point, $p = (x_0, y_0, z_0)$, in each of the two metal plate clusters, plane equations are calculated using a surface normal, $\vec{n} = (a, b, c)$, and point p. The plane equations have the following form:

$$a(x - x_0) + b(y - y_0) + c(z - z_0) = 0$$

which can be normalized to obtain:

$$\frac{a}{d}x + \frac{b}{d}y + \frac{c}{d}z = 1$$

where

$$d = ax_0 + by_0 + cz_0$$

Fourth, the best fit plane for each metal plate is approximated. These planes are used in a later step of the algorithm to extract the contour of the weld along the lower metal plate before the weld is virtually sliced. Figure 7 shows a weld scan and two planes that were fitted to approximate the two metal plates. The best fit plane is approximated using a three dimensional histogram of the unit vector normals

$$\vec{n} = (\frac{a}{d}, \frac{b}{d}, \frac{c}{d})$$

for every point in each of the two clusters.

The most frequently occurring $\vec{n}$ (i.e., the $\vec{n}$ with the largest tally in the histogram) is used as an approximation for the normal to the metal plate.

Virtually Slicing the Weld

In the dental cement procedure described above, weld slices are created by cutting the hardened cement perpendicular to the length of the weld. This is one drawback of the dental molding method because the perpendicular cut is not necessarily the best direction to cut. Rather, the best direction to cut is along the perpendicular to the tangent of the weld profile. Using the virtual slicing method, welds can be sliced along the perpendicular to the tangent to the weld contour, which is the cut that provides the most accurate information for calculating the weld stress concentration factor.

The virtual slices are generated as follows. First, the line of the intersection between the planes approximating the two metal

Copyright © 2010 by ASME

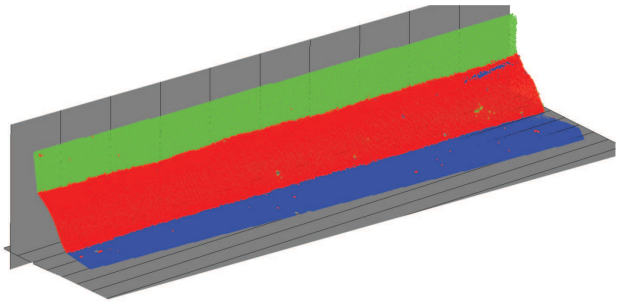

FIGURE 7. TWO PLANES ARE FITTED TO THE 3D POINT DATA TO APPROXIMATE THE TWO METAL PLATES. THE COLORS OF THE POINTS REPRESENT THE CLUSTERS OF POINTS IDENTIFIED BY THE K-MEANS CLUSTERING ALGORITHM (SEE FIGURE 6).

plates is calculated. For each of the two metal plate clusters, the points that are closest to the intersecting line are extracted. By interpolating between these points it is possible to extract the contour line of the weld/plate intersection. Next, a plane is constructed that is perpendicular to both the tangent of the weld contour line and one of the fitted metal plate planes. The algorithm then finds all points that intersect this plane to generate a virtual slice through the weld. A sampling variable determines how many slices to make. Figure 8 shows ten weld slices generated from the 3D point data for the weld scan shown in Figure 7. Each 2D slice is analyzed as described below.

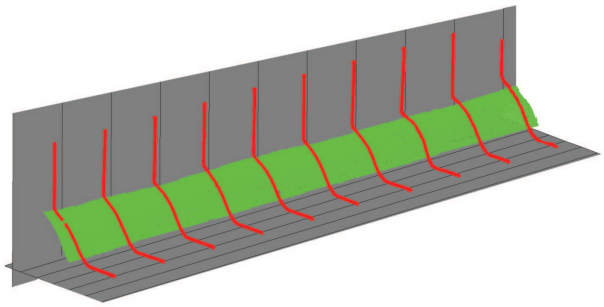

FIGURE 8. TEN VIRTUAL SLICES THROUGH A WELD.

Calculating the Weld Parameters

Two weld parameters are of interest for each 2D weld slice: the weld angle and the radius of the weld at the weld toe. These parameters can be used to determine the integrity of a weld at the location of the weld slice as described above.

The radius parameter of a slice is determined by fitting a circle to the weld toe. The weld toe is located at the junction of the weld and the lower metal plate. To find the weld toe, two regression lines, R_1 and R_2, are calculated for each slice. To filter out some additional noise and especially a small dip in the weld plate right at the beginning of the weld, which is always present due to the physics of welding, the lines are calculated as follows. $R1$ is the regression line that fits the most number of points on the weld plate such that all points are less than ε distance away from the line (where ε is proportional to the minimum distance between two points in the 3D mesh). R_2 is defined similarly by the longest set of consecutive points on the weld. The same procedure that is used to create R_1 can be used to find R_2.

The points from the virtual slice that lie between the two regression lines define the weld toe. Specifically, the weld toe begins at the first point on the weld that deviates from R_1. The first twelve points of the weld toe are used to fit a circle using a 12-point circle fitting algorithm [3]. The radius of the resulting circle defines the weld toe radius.

The weld angle parameter is calculated by finding the angle between R_1 and R_2. Figure 9 shows a virtual weld slice and the two regression lines calculated for it. The points used to fit the circle are also shown along with the circle.

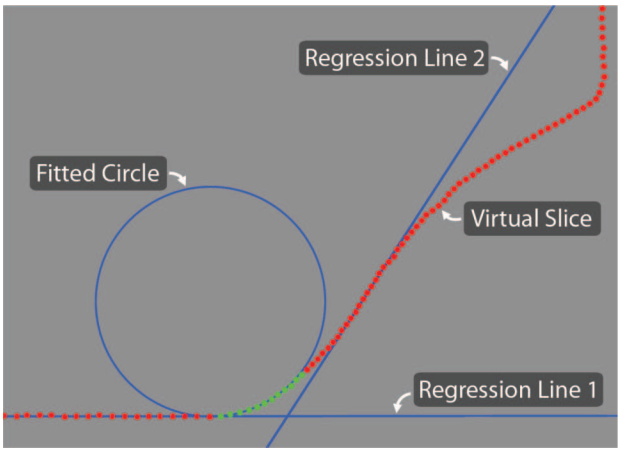

FIGURE 9. FOR EACH WELD SLICE, THE WELD PARAMETERS ARE ESTIMATED BY FITTING TWO REGRESSION LINES AND A CIRCLE TO THE POINTS OF THE SLICE. THE BLUE LINES REPRESENT THE TWO REGRESSION LINES. THE GREEN POINTS ARE THE TWELVE POINTS USED TO FIT A CIRCLE TO THE WELD TOE.

EXPERIMENTAL RESULTS

This section describes the experiments that were used to compare the new virtual weld slicing method with the old method that used dental cement moldings. The geometries of two T-fillet welds were scanned using both methods and results are reported for 20 weld slices.

Copyright © 2010 by ASME

A negative impression of each weld was taken with dental molding. When hardened, the mold was removed from the weld. For each molding, ten sections were cut perpendicular to the weld direction starting 2 mm from the edge of the weld in intervals of 10 mm (see Figure 10). The sections were photographed with a stereo microscope at 20x magnification. Figure 11 shows the profile of one magnified slice of the dental cement.

The weld angle and the radius of each slice were measured from the digital photographs with a software package called Paxit [4]. The weld angle was measured between the top of the horizontal plate and the weld. The radius was calculated using a best fit circle function using 12 points along the weld radius.

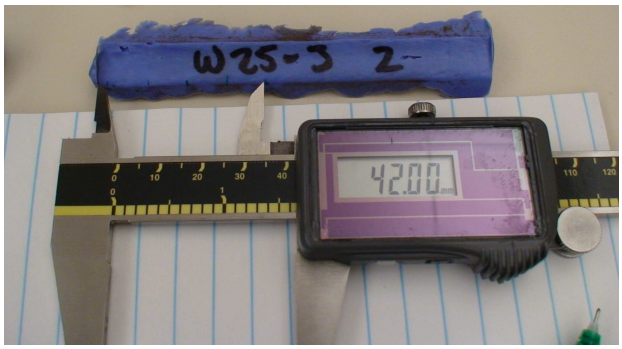

FIGURE 10. THE DENTAL CEMENT MOLDING OF THE WELD IS MARKED AND SLICED AT TEN DIFFERENT LOCATIONS, SPACED 10MM APART. THE SLICES ARE THEN ANALYZED UNDER A MICROSCOPE.

The same welds were also scanned using the ARAMIS 3D camera system. The 3D weld meshes were then virtually sliced using the algorithm described above. For each weld, ten virtual slices were generated at 10 mm intervals in order to match the dental molding slices. The locations of the virtual slices along the weld contour line were matched to the dental cement slices as closely as possible. To accommodate for the limitation of the dental cement method, the slices were made perpendicular to the length of the weld and not perpendicular to the tangent to the contour line.

Tables 1 and 2 show the angle and radius measurements obtained with both the dental cement method and the new method for two sample welds (20 weld slices). The stress concentration factors are also reported. The material thickness, t, was 8mm.

For both welds, the algorithm failed to estimate the parameters for slice 1. This is due to the fact that the 3D mesh data on the weld fringes is usually quite sparse due to the reduced quality of the speckled paint pattern. Because the first slice through the dental cement was taken only 2 mm from the edge of the weld (for both welds), these results were as expected.

To gain further insight into the meaning of the values reported in Tables 1 and 2, the mean difference between the results obtained for K_t^b with the two methods was calculated as follows:

$$\mu = \left(\frac{\sum_{i=2}^{n} |K^b_{t\_virtual_i} - K^b_{t\_dental_i}|}{n-1} \right)$$

where n was equal to 10.

The mean difference for weld 1 and weld 2 was calculated to be 0.029667 and 0.02144, respectively. This difference expressed as a percentage of the mean of $K^b_{t\_dental}$ is 2.2% for weld 1 and 1.6% for weld 2.

The membrane tension factor (K_t^m) was also calculated using data from Tables 1 and 2. The percentage of this relative to the mean of $K^m_{t\_dental}$ is 1.9% for weld 1 and 1.3% for weld 2.

The results indicate that the new virtual slicing method performs similarly to the dental molding procedure. The small differences between the two can be attributed to a number of factors. One reason is that the matching of the dental mold slices and the virtual slices are only approximations of where the dental slices appear to be in the virtual weld scan. This is because the weld scans contain no information about the location of the weld slices. Another factor could be that different circle fitting algorithms were used in the two measurement methods, which may affect the radius calculations.

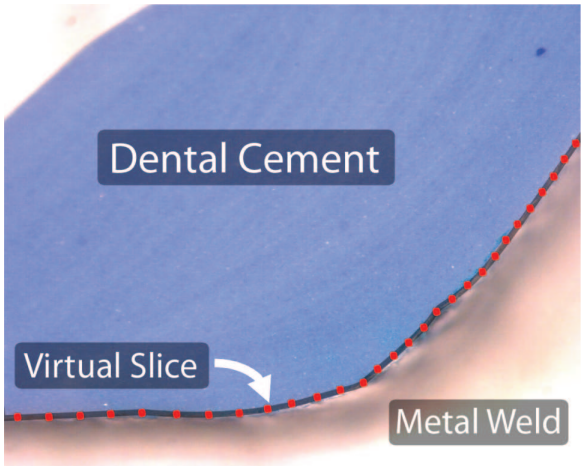

FIGURE 11. THE FIGURE SHOWS VIRTUAL SLICE #7 WHICH HAS BEEN OVERLAID ONTO DENTAL CEMENT SLICE #7. THE RED POINTS REPRESENT THE RAW DATA OF THE VIRTUAL SLICE AND THE BLACK LINE IS AN INTERPOLATED LINE BETWEEN THESE POINTS.

Copyright © 2010 by ASME

TABLE 1. RESULTS FOR WELD #1. THE TABLE COMPARES THE VALUES OBTAINED FOR THE WELD ANGLE (IN RADIANS), THE RADIUS AT THE WELD TOE (IN MM) AND THE BENDING STRESS CONCENTRATION FACTOR K_t^b USING THE TWO DIFFERENT MEASUREMENT METHODS.

	Dental Molding			Virtual Slicing		
#	Angle	Radius	K_t^b	Angle	Radius	K_t^b
1	1.076	2.55	1.31	-	-	-
2	1.160	2.370	1.315	1.217	2.152	1.309
3	0.901	3.964	1.347	0.926	3.122	1.315
4	0.957	3.293	1.329	0.960	2.238	1.275
5	1.035	2.700	1.314	0.989	3.678	1.353
6	1.095	3.115	1.347	1.089	2.673	1.322
7	0.917	2.989	1.307	0.931	4.523	1.376
8	0.983	2.800	1.310	0.973	2.652	1.300
9	0.992	2.651	1.304	0.950	2.897	1.309
10	1.046	3.393	1.351	1.043	2.858	1.324

TABLE 2. RESULTS FOR WELD #2. THE TABLE COMPARES THE VALUES OBTAINED FOR THE WELD ANGLE (IN RADIANS), THE RADIUS AT THE WELD TOE (IN MM) AND THE BENDING STRESS CONCENTRATION FACTOR K_t^b USING THE TWO DIFFERENT MEASUREMENT METHODS.

	Dental Molding			Virtual Slicing		
#	Angle	Radius	K_t^b	Angle	Radius	K_t^b
1	1.028	3.152	1.336	-	-	-
2	1.032	3.834	1.369	0.994	3.003	1.322
3	1.084	1.624	1.254	1.150	1.870	1.281
4	1.041	3.820	1.370	1.036	2.861	1.323
5	0.944	2.318	1.277	0.991	2.396	1.289
6	0.921	3.130	1.315	0.993	2.564	1.299
7	0.940	2.066	1.262	0.907	1.946	1.249
8	0.965	2.210	1.274	0.998	1.933	1.263
9	0.946	3.345	1.329	0.953	3.144	1.322
10	0.927	2.655	1.292	0.981	2.707	1.305

CONCLUSIONS AND FUTURE WORK

This paper described a method for estimating the quality of welds from 3D point data. The method analyzes the geometry of the weld and extracts key parameters that can be used to estimate the stress concentration factor of the weld and thus to infer its quality. The paper described results for T-fillet welds, which show that the method described here produces similar results to the previous method which used dental cement molding.

The viability of this new approach to weld quality testing was estimated by comparing it with measurements produced with the alternative measurement method that uses dental cement. The results show that the new method performs similarly to the current measuring method. With the new method the analysis of the welds can be performed within seconds, while with the old method it took approximately 2 hours to analyze a single weld.

There are a couple of natural extensions of this method that are left for future work. First, the method could be extended to handle welds with different shapes and not just T-fillet welds. This would require a modification to the algorithm to account for the change in weld geometry. Second, different sensors can be used to test new measuring techniques. This could be useful in practical manufacturing applications where an optical camera system might be too cumbersome or too expensive. Finally, some more robust methods might be used to process the 3D mesh data (e.g., [5, 6]) in order to extract the weld slices from the mesh.

REFERENCES

[1] Monahan, C., 1995. "Early fatigue cracks growth at welds". *Computational Mechanics Publications*.

[2] Witten, I. H., and Frank, E., 2005. *Data Mining: Practical machine learning tools and techniques*. Morgan Kaufmann.

[3] Bucher, I., 2008. *Circle Fitting Algorithm (online document)*. http://www.mathworks.com/matlabcentral/fileexchange/5557.

[4] PAX-it, 2008. *Image Database Software*. Available from http://www.paxit.com/ (Date accessed: Feb 2008).

[5] Wu, J., and Kobbelt, L., 2005. "Structure recovery via hybrid variational surface approximation". In Computer Graphics Forum, Vol 24(3) (Eurographics Proceedings), pp. 277–284.

[6] Attene, M., Biasotti, S., and Spagnuolo, M., 2003. "Shape understanding by contour-driven retiling". *The Visual Computer,* ***19***(2–3), May, pp. 127–138.

Copyright © 2010 by ASME